CHEMISTRY OF MATERIALS

ARTICLE

pubs.acs.org/cm

Effect of Substrate Roughness and Feedstock Concentration on Growth of Wafer-Scale Graphene at Atmospheric Pressure

Zhengtang Luo, Ye Lu, Daniel W. Singer, Matthew E. Berck, Luke A. Somers, Brett R. Goldsmith, and A. T. Charlie Johnson*

[†]Department of Physics and Astronomy, University of Pennsylvania, Philadelphia, Pennsylvania 19104, United States

Supporting Information

ABSTRACT: The growth of large-area graphene on catalytic metal substrates is a topic of both fundamental and technological interest. We have developed an atmospheric pressure chemical vapor deposition (CVD) method that is potentially more cost-effective and compatible with industrial production than approaches based on synthesis under high vacuum. Surface morphology of the catalytic Cu substrate and the concentration of carbon feedstock gas were found to be crucial factors in determining the homogeneity and electronic transport properties of the final graphene film. The use of an electropolished metal surface and low methane concentration enabled the growth of graphene samples with single layer content exceeding 95%. Field effect transistors fabricated from CVD graphene made with the optimized process had room temperature hole mobilities that are a factor of 2−5 larger than those measured for samples grown on as-purchased Cu foil with larger methane concentration. A kinetic model is proposed to explain the observed dependence of graphene growth on catalyst surface roughness and carbon source concentration.

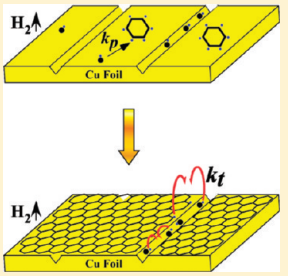

KEYWORDS: graphene, chemical vapor deposition, polymerization, field effect transistor

INTRODUCTION

Graphene has generated enormous interest in the research community because of its great potential for use in electronic devices and other applications.[1] The desire for large-scale production of this material has motivated a number of recent investigations of methods to grow large-area single- (or few-) layer graphene by methods that include ultrahigh vacuum annealing of single crystal SiC,[2,3] and chemical vapor deposition (CVD) on a catalytic metal surface such as Pt, Ru, Ni, or Cu.[4−10] Among the CVD methods, growth on Cu substrates is exceptionally promising because the graphene films thus produced are typically less thick than those grown using other metals.[10,11]

Even thickness fluctuations on the single-atom level are associated with substantial variation in the graphene's properties that are unacceptable for many applications.[12] The thickness uniformity of CVD-grown graphene is thus a critical issue, but reports to date show only limited success in controlling this parameter.[10,11] Here we present an investigation of how the thickness uniformity of the graphene produced using atmospheric pressure CVD can be improved through the use of catalyst films treated with a novel electropolishing process and control of the concentration of the methane feedstock. We find that the use of a very flat, electropolished Cu catalyst surface and extremely low methane concentration enables the growth of a very uniform graphene film. By optimizing the two factors, we obtain graphene samples with single layer content exceeding 95%. Field effect transistors fabricated on such graphene have room temperature hole mobilities that are enhanced by a factor of ∼2−5 compared to samples where these parameters are not optimized. The availability of uniform graphene films will enable the reliable production of large arrays of identical graphene devices, as well as chemically functionalized graphene devices with selected properties. On the basis of the observed dependence of the graphene growth on surface roughness of the catalytic metal film and the carbon source concentration, we propose a preliminary kinetic model for Cu-catalyzed CVD-graphene growth process. Our method also excludes the use of high vacuum in the reaction, which enables a flexible design of the reaction process, and thus is compatible with industrial production and scale-up.

EXPERIMENTAL SECTION

Gases, including methane (purity 99.999%), argon (99.999%), and hydrogen (99.999%) are purchased from GTS-Welco Inc. Cu foil (50 or 25 μm thick) is purchased from Alfa Aesar Inc. or McMaster-Carr Inc. Immediately before graphene growth, Cu foils are cleaned by sonicating in acetic acid for 5 min to remove the oxide layer. Solvents, including 100% ethanol, acetone, chemicals such as $FeCl_3 \cdot 6H_2O$ and HCl, and all other chemicals if not specified are purchased from Thermo Fisher Scientific Inc. All chemicals, if not specified, are used without further purification.

Electropolish of Cu Foil. The copper foil was electropolished using a home-built electrochemistry cell (Figure 2d). Although the electropolishing procedure is based on standard techniques, we are not

Received: October 6, 2010
Revised: December 10, 2010
Published: February 10, 2011

aware of any other report of its use for graphene synthesis. The copper surface was first rough polished with sand paper, then with fine metal polish paste, followed by cleaning in ethanol with sonication. The dried Cu foil was then soldered to a metal wire, and covered with silicone gel on the back, edges, and corners. The Cu foil was then placed into an 800 mL beaker, containing a solution of 300 mL of H_3PO_4 (80%) and 100 mL of poly(ethylene glycol) (PEG, molecular weight 400, from Sigma Aldrich Co.).[13,14] The Cu foil and a large Cu plate were used as work (+) and counter (−) electrode, respectively. A voltage of 1.0−2.0 V was maintained for ∼0.5 h during the polishing process. Immediately after polishing, the Cu foil was washed with large amount of deionized water, with sonication. Any remaining acid on the metal surface was further neutralized by 1% ammonia solution and washing with ethanol, followed by blow-drying with N_2. The silicone gel was then cut or removed. The clean Cu foil was stored in ethanol to prevent later oxidation by air. The smoothing mechanism of the electropolishing process mainly relies on the fact that the current density (and thus the etch rate) varies across the anode surface, and is higher at protruding regions with high curvature (e.g., point A in Figure 2d) compared to other areas (point B); thus the surface of the copper foil is smoothed and leveled by the electropolishing.[13]

Atomic Force Microscopy (AFM). AFM imaging was conducted with tapping mode on DI 3000 (Digital Instruments Inc.).

CVD Growth of Graphene Films. CVD growth of graphene was carried out in a furnace with a 1-in. quartz tube as reaction chamber. A typical growth consisted of the following steps: (1) load the cut Cu foil into the quartz tube, flush the system with Ar (600 sccm)/H_2(10 sccm if not specified) for 10 min, then continue both gas flows at these rates through the remainder of the process; (2) heat the furnace to 800 °C, anneal the Cu foil for 20 min to remove organics and oxides on the surface; (3) raise the temperature to 1000 °C, then start the desired methane flow rate as described later in the text; (4) after reaching the reaction time, push the quartz tube out of the heating zone to cool the sample quickly, then shut off the methane flow. Finally, the sample was unloaded after cooling to room temperature.

PMMA Method for Graphene Film Transfer. This method may be used to transfer the graphene to an arbitrary substrate that is resistant to acetone. A protective thin film of ∼300 nm polymethylmethacrylate (PMMA C4 950, from Microchem Corp.) was spin-coated on graphene film that was grown on the polished side of the Cu growth substrate, followed by baking at 160 °C for 20 min to remove the solvent. Graphene on the back (unpolished) side of the Cu substrate was removed by an oxygen reactive ion etch (RIE) at a power of 45 W for 2−5 min. The sample was then floated on a solution of 0.05 g/mL iron chloride held at 60 °C with the exposed Cu side facing downward. The Cu was gradually etched away over 3 to 10 h. The graphene/PMMA film was washed by transferring into a Petri-dish containing copious deionized water, then floated on 1 N HCl solution and kept for 0.5 h, and transferred to a Petri-dish with deionized water for another wash. The film was then scooped onto an oxidized silicon wafer (300 nm oxide thickness), with the PMMA side up. The sample was gently blown-dry, and heated to 70 °C for ∼30 min to dry. To enable better adhesion of the film to the substrate, another layer of PMMA was applied to the sample surface, followed by baking at 160 °C for 20 min.[15] Finally, the PMMA protective layers were removed by immersing the sample overnight in a large volume of acetone at 55 °C.

PDMS Stamp Method for Graphene Film Transfer. This method using a PDMS stamp was used to transfer the graphene to an arbitrary substrate. Twenty parts of Sylgard 184 prepolymer and 1 part of curing agent were weighed in a plastic cup. The components were fully blended by stirring for 2 min until the mixture was filled with bubbles; the bubbles were then removed by vacuum degassing. The mixture was poured slowly onto the surface of a graphene/Cu foil sample (polished side face up) in a Petri-dish, and the PDMS was then cured in vacuum oven at 70 °C for 1 h. A sharp scalpel was used to cut around the foil. This was followed by removal of the graphene on the back (unpolished) side of the Cu foil by an oxygen RIE at a power of 45 W for 2−5 min. The sample was then floated on 0.05 g/mL iron chloride solution held at 60 °C with the Cu side facing downward. The Cu was etched away over 3 to 10 h, followed by cleaning in copious amount of deionized water, then 1 N HCl solution, then copious amount of deionized water again. After the stamp was gently blown dry, it was placed face down on a substrate, and uniform pressure was applied across the entire surface of the stamp for a few seconds. The stamp was then carefully lifted off, leaving behind the graphene film on a new substrate. An example of a sample transferred by this method is shown in the Supporting Information, Figure S1.

Raman Spectroscopy. Raman spectra of graphene samples on SiO_2/Si or PDMS substrates were obtained using a 514 nm excitation wavelength laser under a 100× objective. The laser power was kept below 4 mW to avoid damage to the sample. Single layer graphene was identified by its unique Raman signatures, that is, it has the Stokes G peak at 1583 cm^{-1} and a single symmetric 2D band around 2700 cm^{-1} (see the Supporting Information, Figure S2 for typical Raman spectrum of single and double layer graphene films).[16]

Single Layer Coverage Calculation. After the contrast of single layer and multilayer regions was identified, the optical image of the graphene was processed with ImageJ software, where multilayer regions (i.e., high contrast region) were outlined. Then the percentage of coverage was derived. An example is shown in the Supporting Information, Figure S4.

Graphene FET Transistor Fabrication Using Electron Beam Lithography. Metal source and drain electrodes, and graphene ribbons were patterned by electron beam lithography using PMMA as e-beam resist. First, optical microscopy was used to locate a single layer graphene film on a 300 nm oxide silicon substrate of prefabricated alignment markers. A 300 nm thick PMMA (PMMA C4 950, from Microchem Corp) film was applied by spin coating using a standard procedure and parameters provided by the manufacturer. Electron-beam patterning was done using a JEOL SEM 6400 operated at 30 kV with a Raith Elphy Plus controller, at an exposure dose of 500 $\mu A/cm^2$, followed by developing in a 1:3 solution of methyl isobutyl ketone (MIBK, Microchem Corp.) and isopropyl alcohol. Chromium (3 nm) and gold (50 nm, both from R.D. Mathis Co.) were then deposited onto the substrate in a thermal evaporator at a pressure of 10^{-7} Torr. The deposited films were lifted off in an acetone bath for 12 h at 70 °C and rinsed extensively with isopropyl alcohol. With the electrical contacts thus fabricated, another electron beam lithography step identical to the one just described and an oxygen RIE were used to pattern isolated channels of graphene connecting each pair of source and drain electrodes.

Electronic Transport Measurements. Devices were created in three-terminal transistor geometry, where the p++ doped silicon wafer was used as a global back gate. Source, drain, and gate electrodes were contacted using individual probes in a custom-made, small-signal probe station, controlled using Labview. A data acquisition card (National Instruments) was used to output source-drain voltage, and a Keithley 6517A current meter was used to read the source-drain current and to output the gate voltage.

RESULT AND DISCUSSION

Figures 1a−b are optical images of an untreated Cu foil under low and high magnification, respectively. The Cu surface shows a directional texture consisting of many parallel lines with spacing on the order of tens of micrometers. By adjusting the focal plane of the optical microscope, we have verified that these grooves in the copper have a concave cross section, as reported by others.[10] These striations are thought to be produced during the flat rolling

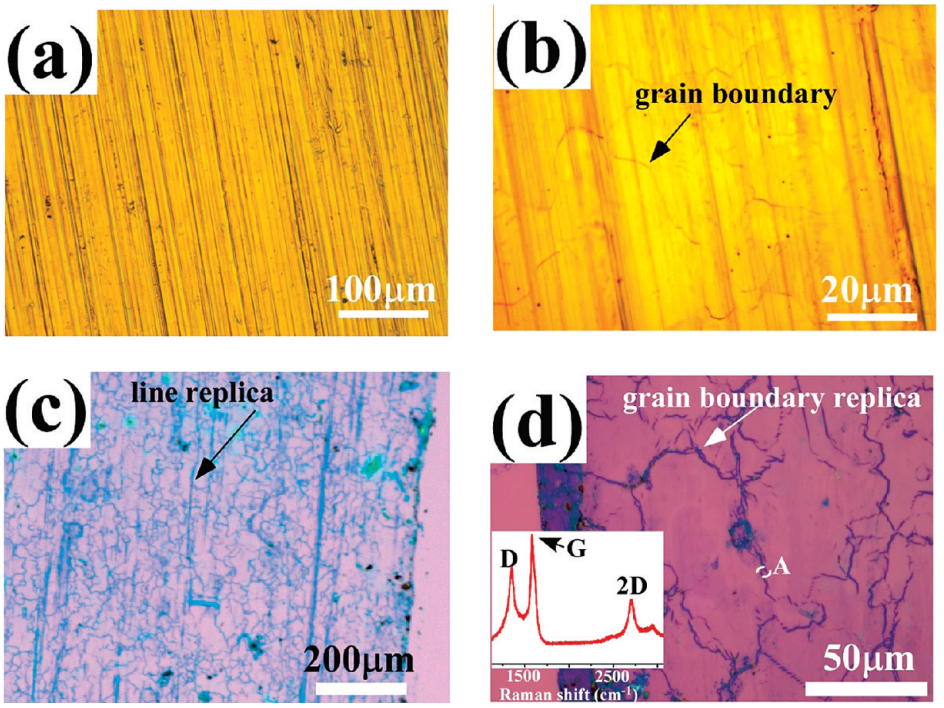

Figure 1. Optical images of (a, b) unpolished Cu foil and (c, d) CVD-graphene film grown on the Cu foil after transfer to an oxidized silicon substrate. Inset: Raman spectrum taken at point A in Figure 1d.

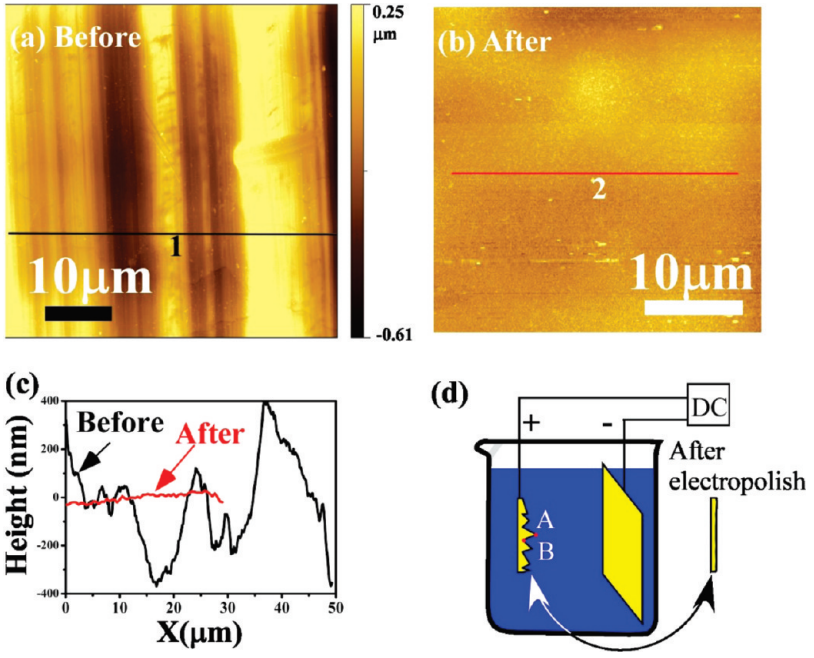

Figure 2. AFM topography images of Cu foil (a) before and (b) after electropolishing, shown with the same height color scale. (c) Line profiles of positions indicated in (a) and (b). (d) Schematic diagram of the electropolishing setup.

process used to fabricate the Cu foil, with the lines running parallel to the shear/drawing direction.[17] Figure 1b also shows the presence of grains (typical size ~50 μm) and grain boundaries on the Cu surface.

Figure 1c and 1d are optical micrographs of graphene films that were grown by CVD on the same copper foil that is shown in Figure 1a and 1b, and then transferred to an oxidized silicon wafer using a PMMA-based method.[9,11] On the basis of a careful comparison between the texture of the transferred graphene film (Figure 1c) and the Cu foil surface texture (Figure 1a), we conclude that the latter is a replica of the former, where the thick part of the graphene corresponds to the deep trenches seen in the Cu surface. On the basis of a similar analysis of the higher magnification images (Figure 1b and 1d), we conclude that the

dx.doi.org/10.1021/cm1028854 |*Chem. Mater.* 2011, 23, 1441–1447

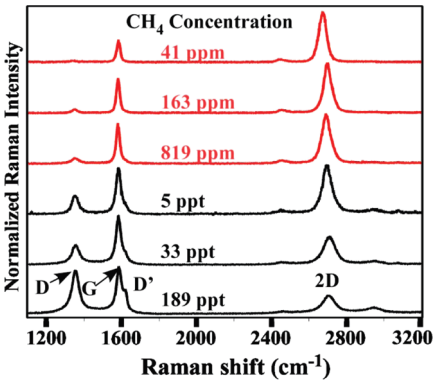

Figure 3. Raman spectra of graphene grown on Cu foil by CVD and then transferred to a 300 nm oxide silicon substrate using PMMA method (see full text for details). Raman spectra of graphene grown on unpolished and electropolished Cu foil are depicted as black and red curves, respectively.

finer grain boundary structures of the Cu foil (Figure 1b) also lead to thickness variations in the graphene film.

Raman measurements of the graphene film regions that replicate the grain boundary and striated Cu regions indicate that carbon atoms in these areas are mostly in disordered sp^3-bonded networks as evidenced by the high intensity of the D band (~1350 cm^{-1}) and the very weak 2D band (~2700 cm^{-1}), shown in the inset of Figure 1d. This observation that disordered carbon forms at grain boundaries of the catalytic Cu substrate differs from the highly ordered, multilayer graphene structures that form in grain boundary regions when Ni is used as the catalytic film, as reported by others[18,19] and verified by us (Raman spectrum of Ni-catalyzed graphene grown in a grain boundary region is shown in the Supporting Information, Figure S3). The formation of ordered graphene multilayers at grain boundaries on Ni catalytic substrates has been attributed to the fact that carbon atoms are attracted to step edges and other surface irregularities where they passivate metal edge atoms and nucleate graphene growth.[17,18] The observations reported here suggest that the mechanism of graphene growth on Cu foil differs significantly from the growth mechanism on Ni, with the growth of ordered graphene on Cu being less dependent on nucleation at step edges and/or surface irregularities.

The correlation of graphene thickness variation with the topography of the catalytic Cu foil motivated the idea that smoothing the Cu through polishing would lead to more uniform and better quality graphene. Figures 2a−b are AFM images illustrating how electropolishing greatly reduces the Cu foil surface roughness. The surface of the as-purchased foil (Figure 2a) is very rough, showing trenches several hundred nanometers in depth and general texturing consistent with what is seen in the optical micrographs (Figure 1a−b). After electropolishing, the roughness of the Cu surface is reduced (Figure 2b) by a factor of 10−30, as evidenced by the line scans in Figure 2c.

Before the discussion of CVD-graphene growth on electropolished Cu foil, we address the issue of methane concentration, which we have also found to be an important factor in controlling the graphene thickness and homogeneity. Figure 3 shows Raman spectra from graphene samples that were grown using different methane concentrations and then transferred by the PMMA method onto an oxidized silicon substrate. The three higher methane concentration samples (black curves in Figure 3) were grown on unpolished Cu samples, while the other three lower methane concentrations were grown on polished Cu foil (red curves). A growth time of 40 min was used for the samples grown at the two lowest methane concentrations (41 ppm and 163 ppm) to enable high graphene coverage, while the growth time for each of the other samples was 10 min. All plotted spectra are the average of 5 spectra taken at regions deemed to be the most uniform and thinnest parts of the film to avoid Raman changes associated with variation in the graphene thickness.

Three major bands in the Raman spectrum of graphitic materials are typically used to infer structural information: (1) D-("disorder") band at ~1350 cm^{-1}; as well as D′ band, that is, sideband at ~1620 cm^{-1}; the relative intensity of these peaks reflects the degree of disorder, or relative sp^3 carbon content, in the carbon structure; (2) G-band at ~1583 cm^{-1}; (3) 2D or G′ band at ~2670 cm^{-1}, which is the second harmonic of the D band. Single layer graphene is known to exhibit a single highly symmetric 2D band, while the 2D band for two- or few-layer graphene exhibits an asymmetric peak consisting of multiple Lorentzian components.[16] In addition, the relative intensity of the 2D and G bands is an indication of the film thickness of an undoped graphene sample; single layer graphene has higher 2D intensity (typically $I_{2D}/I_G > 2$).[11]

We find that when CVD growth is done with a methane concentration greater than 5 ppt, no sizable single layer graphene regions are observed, and the sample has a large D band and significant D′ sideband. We conclude that when high methane concentration is used, thick graphitic regions with significant sp^3 defect content are formed on the Cu foil surface. Moreover, we find that the defect density, as reflected by the relative D-band intensity, decreases as the methane concentration is reduced, and that this is accompanied by a significant decrease in the average thickness of the graphene film. This very strong dependence of the growth process on the reactant concentration leads us to the conclusion that growth kinetics are a critical factor in determining the properties of the graphene in the case of Cu-catalyzed growth.

Figure 4a is an optical micrograph of a graphene film synthesized with 41 ppm methane on electro-polished Cu foil. Of the Raman spectra taken from 30 random locations, only two types of spectra were seen, that is, Raman spectra similar to those at spot A and B that resemble those collected from a single and double layer of exfoliated pristine graphite,[16] respectively (see the Supporting Information, Figure S2 for Raman spectra of single and double layer graphene generated by mechanical exfoliation). As shown in the insets of Figure 4b, the spectrum at point A has a single symmetric 2D band around 2700 cm^{-1}, as expected for single layer graphene, while the 2D peak at point B is a convolution of four components, as expected for bilayer graphene.[16] The optical contrast of these two regions in Figure 4a is also consistent with that known to exist for single and bilayer graphene on 300 nm SiO_2/Si.[1] On the basis of a computerized analysis of optical micrographs of the sample, we estimate that single layer graphene constitutes ~95% of the sample grown in an atmosphere containing 41 ppm methane (see Supporting Information, Figure 4 for details). A uniform graphene film was formed on the entire copper surface, regardless of the grain orientation, suggesting that the graphene growth is not sensitive to the Cu crystal orientation. A small amount of double or multiple layer regions still exists, possibly because of the finite roughness of the catalytic surface limited by the electropolishing process. Graphene grown under identical conditions on

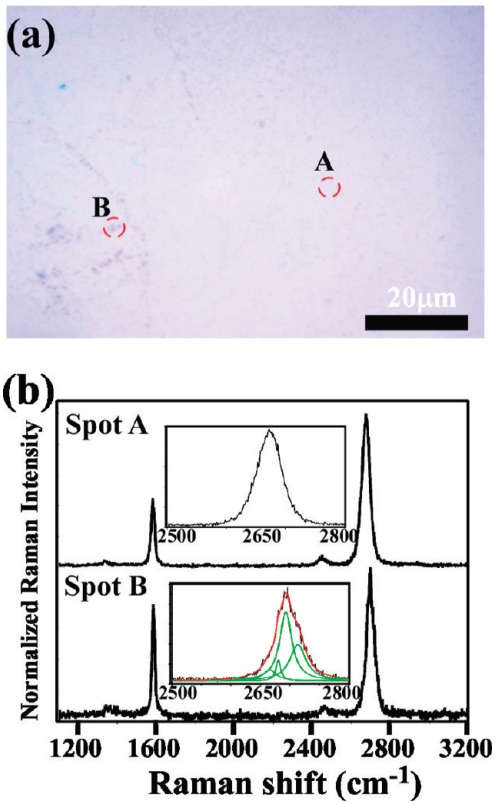

Figure 4. (a) Optical micrograph of graphene grown on electropolished Cu with a methane feedstock concentration of 41 ppm and then transferred to an oxidized Si substrate. (b) Raman spectra taken at spots A and B in Figure 4(a). Insets in Figure 4(b) show details of the 2D band. The spectrum at point A is a single Lorentzian, indicating that this region is single layer graphene, while the 2D peak at point B is a convolution of four components, as expected for double layer graphene.

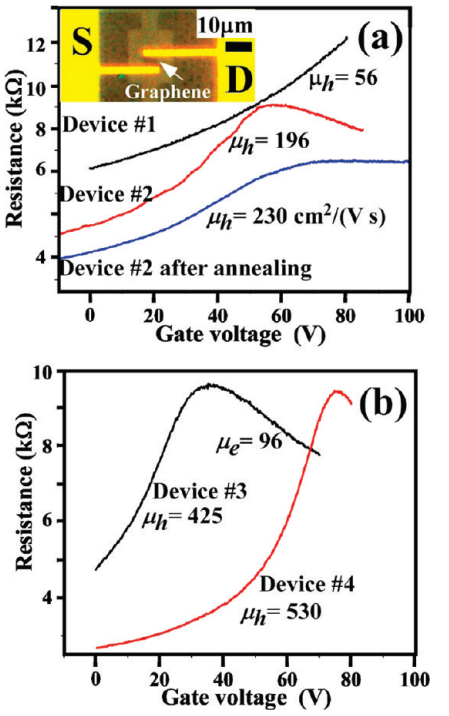

Figure 5. Resistance as function of gate voltage for typical graphene FET devices fabricated from single layer graphene grown on (a) as-obtained and (b) electropolished Cu foil. Inset: optical micrograph of a graphene FET device.

as-received Cu foil showed significantly greater bilayer and multilayer content (Supporting Information, Figure 5).

Figures 5a−b are plots of the resistance as a function of gate voltage for typical graphene FET devices fabricated on single layer graphene grown on as-received and electropolished Cu foil, respectively, with a methane concentration of 41 ppm. The room temperature hole mobility for graphene samples grown on electropolished Cu foil (400−600 cm^2/V s) is significantly enhanced over the mobility of graphene grown on as-received Cu foil (50−200 cm^2/V s). This observation is consistent with the hypothesis that carrier scattering is associated with disordered carbon regions that form in the graphene film because of surface roughness of the Cu foil. The disordered carbon content is significantly reduced when polished Cu is used as the catalyst, and further reduced by the use of a low methane concentration in the growth atmosphere. The observed hole mobility is less than the value ∼2000−3000 cm^2/V s found for exfoliated ("Scotch tape") graphene[20,21] which may reflect a higher defect level in our CVD graphene compared to graphene derived from bulk graphite.[11] Various values of hole mobility have been reported for graphene grown by low pressure CVD, ranging from 500 cm^2/V s to more than 5000 cm^2/V s,[22,23] making it difficult to assess the impact of growth pressure on material quality. One way to further increase the conductivity and mobility of the devices is by sample annealing.[20] As shown in Figure 5a, the resistance versus gate voltage characteristic measurement on device 2 shows that the mobility of the device significantly enhanced by annealing, while its overall resistance is reduced.

Two mechanisms have been suggested[24] to understand the formation of graphitic carbon on metal surfaces: (1) dissolution−precipitation, or segregation, process, where carbon is solubilized in the metal film and then precipitates out in a low energy form upon cooling; and (2) CVD process, which mainly includes adsorption and disassociation of precursor molecules on the surface where the graphitic material grows, with minimal dissolution of carbon in the metal film.

Because of the extremely low solubility of carbon in Cu,[25] it is more likely that graphitization is dominated by the CVD process for Cu-catalyzed growth. Moreover, recent first principles modeling of graphene growth on different metals shows that the Cu-catalyzed process differs strongly from the growth on other metals.[26,27] First principles calculations indicate that, in contrast to graphene growth on other metals, Cu-catalyzed graphene growth is unique in that surface irregularities (i.e., metal step edges and other defects) do *not* serve as centers for carbon adsorption and growth nucleation.[26] Instead, nucleation is found to proceed readily on the crystal plane. Carbon adatoms are found to interact mainly with free-electron-like surface states in Cu, while they strongly bind to other metal surfaces through orbital hybridization,[26] leading to a comparatively weak surface diffusion barrier on the Cu surface.[26,27] A direct consequence of this difference is that carbon−carbon interactions dominate the growth on Cu, since carbon dimers are more stable than isolated C adatoms by over 2 eV,[26] while carbon−carbon coupling is energetically unfavorable on other metal surfaces.

The high reactivity and relative independence to the environment characteristic of hot carbon adatoms on Cu closely resemble the properties of carbon free radicals.[26−28] Indeed,

dx.doi.org/10.1021/cm1028854 |*Chem. Mater.* 2011, 23, 1441–1447

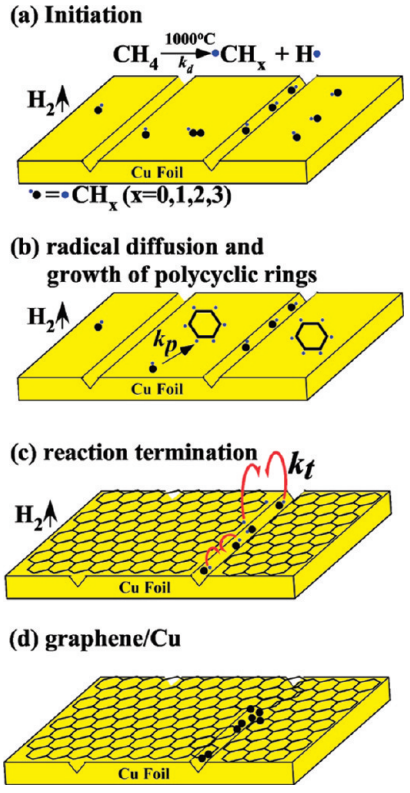

Figure 6. Proposed reaction pathways, analogous to free radical polymerization, for graphene growth on uneven Cu metal surface during CVD. (a) dissociation of hydrocarbon on heated Cu surface; (b) nucleation and growth of graphene; (c) reaction termination when two active center react with each other; (d) final graphene with turbostatic structures and amorphorous carbon because of surface roughness.

there is an extensive body of literature indicating that several different radical species are formed on metal surfaces when hydrocarbons are heated to high temperature,[29−31] and a more recent report supporting the conjecture that graphene growth can proceed from methyl radicals.[32] Consequently, the fundamental question that arises is whether the hot adatom nucleation and graphene growth on the copper surface can be modeled as free radical chain polymerization involving the following three stages:[33] (1) initiation, (2) propagation, and (3) reaction termination (Figure 6). In the initiation stage, methane adsorbs on the Cu surface at elevated temperature, and hydrogen atom(s) dissociate from the methane molecules, yielding reactive carbon radicals on both the uniform crystal terraces and any surface irregularities (step edges, large scale striations, etc.). In all stages of the growth, hydrogen radicals released by hydrocarbon species will recombine and form hydrogen gas molecules. In the chain (plane) growth stage, surface carbon radicals diffuse along the Cu surface and form polycyclic hydrocarbon structures, whose reactive edge atoms serve as growth seeds for the resulting graphene film. Carbon radicals on smooth film regions diffuse readily, enabling the formation of a graphitic sp^2 bonded network. In contrast, radicals trapped in "valleys" on the metal surface and other irregularities lack the surface mobility required to form large-scale graphene structures, leading to the formation of defected, sp^3 bonded networks as the reaction terminates.[26] Since the molecular weight of the formed polymer (graphene in this case) is proportional to the ratio of the rate of chain (here, plane) growth[33] (R_p with k_p as chain propagation constant) to reaction termination (R_t with k_t as chain termination constant), that is, graphene size $\sim k_p/k_t$, one expects that only small graphene fragments or amorphous carbon will form in surface irregularities associated with grain boundaries and surface textures. Once a completely intact single layer graphene film forms on the Cu surface, lack of access to the catalytic surface will lead to suppression of methane into free radicals; this leads to a significant change in the deposition mechanism, inhibiting the formation of a second graphene layer.

CONCLUSION

In conclusion, we presented a method to grow uniform, large-size graphene film using CVD on electropolished Cu foil. A very flat surface morphology and low methane concentration in the CVD atmosphere were shown to be crucial factors leading to enhanced homogeneity and electronic transport properties of the resulting graphene material. By tuning these parameters we have been able to obtain graphene samples with single layer content exceeding 95%. Field effect transistors fabricated on such graphene samples show room temperature hole mobilities enhanced by a factor of 2−5 compared to those grown on unpolished Cu substrates. On the basis of a kinetic model for graphene growth inspired by free radical chain polymerization, we propose that the termination stage of the growth is dominated by high concentration of trapped radicals in the valleys of the Cu surface compared to the flat regions, causing the valleys to contain larger amounts of amorphous or turbostatic carbon and graphene fragments.

ASSOCIATED CONTENT

Supporting Information. Pictures of PDMS-transferred graphene film, Raman spectra of exfoliated graphene, Raman spectra of graphene film grown on Ni. This material is available free of charge via the Internet at http://pubs.acs.org.

AUTHOR INFORMATION

Corresponding Author
*E-mail: cjohnson@physics.upenn.edu.

ACKNOWLEDGMENT

We thank Dr. Rui Zhang, Ms. Jinnie George, and Prof. Stanko R. Brankovi for helpful discussions on the electropolishing procedure. This work was supported by the Nano/Bio Interface Center through the National Science Foundation NSEC DMR08-32802.

REFERENCES

(1) Novoselov, K. S.; Geim, A. K.; Morozov, S. V.; Jiang, D.; Zhang, Y.; Dubonos, S. V.; Grigorieva, I. V.; Firsov, A. A. *Science* **2004**, *306*, 666–669.

(2) Berger, C.; Song, Z.; Li, X.; Wu, X.; Brown, N.; Naud, C.; Mayou, D.; Li, T.; Hass, J.; Marchenkov, A. N.; Conrad, E. H.; First, P. N.; de Heer, W. A. *Science* **2006**, *312*, 1191–1196.

(3) Emtsev, K. V.; Bostwick, A.; Horn, K.; Jobst, J.; Kellogg, G. L.; Ley, L.; McChesney, J. L.; Ohta, T.; Reshanov, S. A.; Roehrl, J.; Rotenberg, E.; Schmid, A. K.; Waldmann, D.; Weber, H. B.; Seyller, T. *Nat. Mater.* **2009**, *8*, 203–207.

(4) Marchini, S.; Gunther, S.; Wintterlin, J. *Phys. Rev. B* **2007**, *76*, 075429.

(5) Loginova, E.; Bartelt, N. C.; Feibelman, P. J.; McCarty, K. F. *New J. Phys.* **2008**, *10*, 093026.
(6) Sutter, P. W.; Flege, J.-I.; Sutter, E. A. *Nat. Mater.* **2008**, *7*, 406–411.
(7) Yu, Q.; Lian, J.; Siriponglert, S.; Li, H.; Chen, Y. P.; Pei, S.-S. *Appl. Phys. Lett.* **2008**, *93*, 113103-3.
(8) Reina, A.; Jia, X.; Ho, J.; Nezich, D.; Son, H.; Bulovic, V.; Dresselhaus, M. S.; Kong, J. *Nano Lett.* **2009**, *9*, 30–35.
(9) Kim, K. S.; Zhao, Y.; Jang, H.; Lee, S. Y.; Kim, J. M.; Kim, K. S.; Ahn, J.-H.; Kim, P.; Choi, J.-Y.; Hong, B. H. *Nature* **2009**, *457*, 706–710.
(10) Li, X.; Cai, W.; An, J.; Kim, S.; Nah, J.; Yang, D.; Piner, R.; Velamakanni, A.; Jung, I.; Tutuc, E.; Banerjee, S. K.; Colombo, L.; Ruoff, R. S. *Science* **2009**, 1171245.
(11) Cao, H.; Yu, Q.; Jauregui, L. A.; Tian, J.; Wu, W.; Liu, Z.; Jalilian, R.; Benjamin, D. K.; Jiang, Z.; Bao, J.; Pei, S. S. S.; Chen, Y. P. *arXiv.org, e-Print Arch.* **2009**, 1–19.
(12) Cresti, A.; Nemec, N.; Biel, B.; Niebler, G.; Triozon, F.; Cuniberti, G.; Roche, S. *Nano Res.* **2008**, *1*, 361–394.
(13) Tegart, W. J. M. *The Electrolytic and Chemical Polishing of Metals in Research and Industry*; Pergamon Press: London, 1956.
(14) Shivareddy, S.; Bae, S.-E.; Brankovic, S. R. *ECS Trans.* **2008**, *13*, 21–32.
(15) Li, X.; Cai, W.; Colombo, L.; Ruoff, R. S. *Nano Lett.* **2009**, *9*, 4268–4272.
(16) Ferrari, A. C.; Meyer, J. C.; Scardaci, V.; Casiraghi, C.; Lazzeri, M.; Mauri, F.; Piscanec, S.; Jiang, D.; Novoselov, K. S.; Roth, S.; Geim, A. K. *Phys. Rev. Lett.* **2006**, *97*, 187401.
(17) Hirsch, J.; Lucke, K. *Acta Metall.* **1988**, *36*, 2863–82.
(18) Yudasaka, M.; Kikuchi, R.; Matsui, T.; Ohki, Y.; Baxendale, M.; Yoshimura, S.; Ota, E. *Thin Solid Films* **1996**, *280*, 117–123.
(19) Johansson, A.-S.; Lu, J.; Carlsson, J.-o. *Thin Solid Films* **1994**, *252*, 19–25.
(20) Dan, Y.; Lu, Y.; Kybert, N. J.; Luo, Z.; Johnson, A. T. C. *Nano Lett.* **2009**, *9*, 1472–1475.
(21) Novoselov, K. S.; Jiang, D.; Schedin, F.; Booth, T. J.; Khotkevich, V. V.; Morozov, S. V.; Geim, A. K. *Proc. Natl. Acad. Sci.* **2005**, *102*, 10451–10453.
(22) Li, X.; Magnuson, C. W.; Venugopal, A.; An, J.; Suk, J. W.; Han, B.; Borysiak, M.; Cai, W.; Velamakanni, A.; Zhu, Y.; Fu, L.; Vogel, E. M.; Voelkl, E.; Colombo, L.; Ruoff, R. S. *Nano Lett.* **2010**, *10*, 4328–4334.
(23) Huang, P. Y.; Ruiz-Vargas, C. S.; Zande, A. M. v. d.; Whitney, W. S.; Levendorf, M. P.; Kevek, J. W.; Garg, S.; Alden, J. S.; Hustedt, C. J.; Zhu, Y.; Park, J.; McEuen, P. L.; Muller, D. A. *Nature* **2011**, *469*, 389–392.
(24) Irving, S. M.; Walker, P. L. *Carbon* **1967**, *5*, 399.
(25) Okamoto, H. *Phase diagrams for binary alloys: A desk handbook*; ASM International: Materials Park, OH, 2000.
(26) Chen, H.; Zhu, W.; Zhang, Z. *Phys. Rev. Lett.* **2010**, *104*, 186101.
(27) Yazyev, O. V.; Pasquarello, A. *Phys. Rev. Lett.* **2008**, *100*, 156102/1–156102/4.
(28) Yazyev, O. V.; Pasquarello, A. *Phys. Status Solidi B* **2008**, *245*, 2185–2188.
(29) Zhu, X. Y.; White, J. M. *Surf. Sci.* **1989**, *214*, 240–56.
(30) Marinov, N. M.; Pitz, W. J.; Westbrook, C. K.; Castaldi, M. J.; Senkan, S. M. *Combust. Sci. Technol.* **1996**, *116−117*, 211–287.
(31) Ranzi, E.; Sogaro, A.; Gaffuri, P.; Pennati, G.; Westbrook, C. K.; Pitz, W. J. *Combust. Flame* **1994**, *99*, 201–11.
(32) Wellmann, R.; Bottcher, A.; Kappes, M.; Kohl, U.; Niehus, H. *Surf. Sci.* **2003**, *542*, 81–93.
(33) Odian, G. *Principles of Polymerization*, 4th ed.; Wiley-Interscience: New York, 2004.